Low Complexity Positioning System for Indoor Multipath Environments

Heinrich Luecken and Armin Wittneben
Communication Technology Laboratory, ETH Zurich, 8092 Zurich, Switzerland
{lueckenh, wittneben}@nari.ee.ethz.ch

***Abstract*—In this paper, we consider localization based on the Time-of-Arrival (ToA) of Ultra-Wideband (UWB) impulse radio pulses. We present a receiver structure for ToA estimation, which can be implemented with very low complexity and low power consumption. Standard approaches for ToA estimation of UWB pulses require very high speed A/D conversion, which makes them impractical for implementation. Although ToA estimation based on phase estimation of narrowband signals circumvents that problem, the estimation performance suffers strongly from multipath propagation. We propose to combine the advantages of both techniques by performing spectral estimation at the output of a UWB energy detection receiver. This system benefits from resolvability of multipath components due to a large signaling bandwidth, but requires only low sampling rates. The impact of bandwidth on the ToA estimation accuracy is derived analytically and a closed form approximation of the estimation variance for a multipath channel is given. Moreover, we present a performance evaluation based on measured channels and show that accuracy up to 20 cm can be reached in strong multipath environments.**

I. Introduction

The development of affordable 3-D motion tracking technology is key enabler for many applications in robotics, industrial automation or entertainment. In this paper, we aim for a low complexity, low power and low cost positioning system that still offers reasonable localization accuracy, as e.g. necessary for motion tracking of persons or body parts. The desired application environment is indoor and is characterized by rather short distances of up to about 10 m, as e.g. common for wireless personal area networks (WPAN) or body area networks (BAN).

In terms of low complexity and power consumption, narrowband positioning systems, which are based on phase measurements, are the method of choice (e.g. [1], [2]). In an indoor environment, the multipath propagation is a major source of impairment however and leads to substantial positioning errors [3]. Ultra-Wideband (UWB) positioning systems can resolve the multipath and are as such much more robust [4]. They require huge sampling rates however and are thus not directly suitable for our application regime. The key idea of this paper is to combine aspects of narrowband and UWB positioning such that the advantages of both approaches are captured.

Before we summarize the contribution of the paper, a short overview of related work in UWB and narrowband ToA estimation is given. For a comprehensive review of indoor position location techniques, the reader is referred to [3] and [4]. Reference [5] provides an overview of timing and ToA estimation for UWB receivers. In [6], the generalized maximum-likelihood estimator for the direct path in presence of multipath components is presented and analyzed. Reference [7] presents threshold-based ToA estimators. Even though these estimators are superior in terms of performance, they are impractical for implementation, because they require Nyquist sampling of the received signal. When using the whole UWB bandwidth according to FCC regulation this would require an analog-to-digital conversion (ADC) of at least 15 GHz sampling rate. By using noncoherent receivers, the sampling rate can be decreased, but is still in the gigahertz range [8], [9]. Contrariwise, narrowband positioning systems based on phase measurements including carrier phase-based differential GPS (DGPS) can be implemented requiring ADC and digital processing only with about or less than 2 MHz sampling rate [2]. However, when applied in a multipath indoor environment the phase of the narrowband signal becomes random. The single multipath contributions are not resolvable which leads to substantial positioning errors.

In this paper, we propose and analyze a hybrid system, which combines elements of UWB and narrowband positioning. We assume a UWB impulse radio (IR) source, which generates either a dedicated training sequence or a data signal. Thus, our system can be implemented either as stand-alone positioning system or as low complexity add-on to a low complexity UWB-IR communication system. For complexity reasons, we consider a non-data-aided ToA estimator without any channel state information. Specifically, the received signal is processed by a standard analog energy detector front end. In the add-on scenario, this front end is typically present anyway for data detection. The ToA specific part of the receiver then consists of a narrowband quadrature demodulator, low-pass and low rate ADC. Our ToA estimator is based on the observation, that the energy detector output signal has a periodic component and thus discrete spectral lines at multiples of the symbol frequency. The ToA estimate is deduced from the complex amplitude of the spectral line at symbol frequency. In this respect, the estimator is closely related to the classical square timing recovery [10].

Besides the basic idea to combine UWB and narrowband positioning, the main contribution of the paper is an analysis of this estimator under multipath propagation. Simulation results of the estimator performance for simulated and measured channel impulse responses confirm the theory and highlight the improved multipath robustness.

The remainder of the paper is structured as follows. In

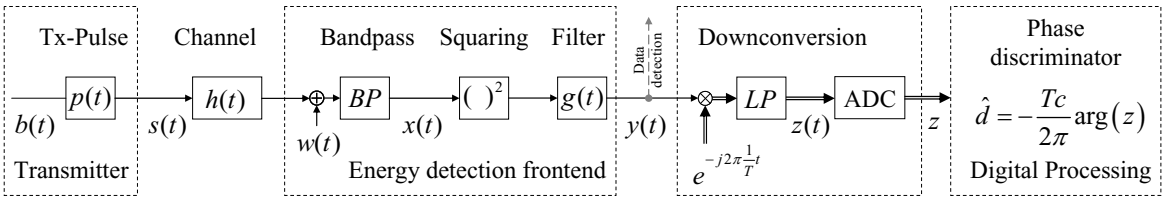

Fig. 1. Block diagram of transmitter, channel and receiver

Section II, the considered system model is described. In Section III, the input/output relation of the proposed receiver structure is derived. The impact of multipath propagation is analyzed in Section IV. Simulation results on the estimator performance are given in Section V.

II. System Model

We consider a radio transmitter that transmits a sequence of modulated pulses $p(t)$, i.e. in Fig. 1 we have

$$b(t) = \sum_k a_k \delta(t - kT).$$

The pulse repetition period is denoted by T. For the add-on scenario the transmit symbols a_k carry the data stream. In the case of Binary On/Off Keying (B-OOK), the mapping of the input bit to the transmit symbol is given by "0" $\mapsto 0$ and "1" $\mapsto (\pm 1)$. Note that the polarity of the "1"-symbol is chosen randomly to avoid discrete spectral lines in the transmit signal spectrum. Otherwise, the FCC rules for UWB could not be exploited to the full extend. For Binary Pulse Position Modulation (B-PPM) in turn each input bit corresponds to two output symbols, i.e. we use the mapping "0" $\mapsto (\pm 1, 0)$ and "1" $\mapsto (0, \pm 1)$. We again use random pulse amplitudes (± 1), which are independent and identically distributed (i.i.d.) such that $\mathsf{E}[a_k] = 0$ and spectral lines are avoided. For the stand-alone scenario the symbols a_k do not carry a data stream and are i.i.d. for the same reason. Note that in all cases the ToA estimator does not require knowledge of the transmit symbols a_k.

The transmit signal is given by

$$s(t) = \sum_{k=-\infty}^{\infty} a_k p(t - kT),$$

which is transmitted over the propagation channel with impulse response $h(t)$. At the receiver, the signal is perturbed by additive white Gaussian noise $w(t)$. First, the signal is applied to an energy detector. It consists of bandpass filter, a squaring device and a post detection filter with impulse response $g(t)$. The output of the energy detector $y(t)$ is then downconverted by mixing with frequency $1/T$. Note that all this processing can be done in analog with low complexity. In the digital part, the complex value of the DC ($f = 0$) component of the low-pass output is estimated. Thus, the sampling rate of the ADC is determined by the desired number of ToA estimates per second. It is independent of other system parameters, in particular the pulse rate and the system bandwidth.

The distance estimate is obtained by computing the phase according to

$$\hat{d} = -\frac{Tc}{2\pi}\arg(z), \tag{1}$$

where $\arg(\cdot)$ gives the argument of the complex number. For the analysis of the distance estimation, we impose the following assumptions:

- The local oscillator can produce the exact frequency $1/T$ and does not suffer from any phase noise or frequency offset.
- There is no interference from other nodes or other wireless systems.
- The base pulse $p(t)$ and impulse responses of $g(t)$, the bandpass and low-pass are even, i.e. their spectra are real.

Eventually, to calculate the position, the nodes may be able to synchronize, i.e. from ToA estimation it may be possible to derive the time-of-flight, thus the distance and further the position by multilateration or joint position and clock offset estimation, as e.g. presented in [1].

III. Input Output Relation

First, we derive the input/output relation of the considered receiver structure. The signal at the output of the bandpass filter is given by

$$x(t) = \sum_{k=-\infty}^{\infty} a_k q(t - kT) + n(t),$$

where $n(t)$ denotes the band-limited noise and $q(t)$ the receive base pulse, which comprises transmit pulse shape, channel impulse response and bandpass filter.

After squaring and post-detection filtering by the filter with impulse response $g(t)$, we obtain the signal $y(t)$, see Fig. 1. It consists of a periodic component $y_p(t)$ and a non-periodic component $y_{\text{NP}}(t)$, i.e. $y(t) = y_p(t) + y_{\text{NP}}(t)$. The periodic component $y_p(t)$ yields the discrete spectral lines, which we are interested in. It is given by

$$\begin{aligned} y_p(t) \mathrel{\hat{=}} \mathsf{E}[y(t)] &= \mathsf{E}\left[g(t) * \left(\sum_{k=-\infty}^{\infty} a_k q(t - kT) + n(t) \right)^2 \right] \\ &= g(t) * \sum_{k=-\infty}^{\infty} \mathsf{E}[a_k^2] \cdot q^2(t - kT) + \sigma_g^2, \end{aligned} \tag{2}$$

where the constant mean of the squared noise term is denoted by σ_g^2. Eq. (2) holds if at least one of the following conditions

applies:

$$\text{i)} \qquad \mathsf{E}[a_k a_l] = \delta[k-l], \tag{3}$$

$$\text{ii)} \qquad q(t) \cdot q(t-kT) = 0, \forall k \neq 0. \tag{4}$$

The first condition holds for both the add-on and the stand-alone scenario, if the symbol mapping is done as described in Section II. Eq. (4) implies non-overlapping receive impulses. This condition is frequently met in low to medium data rate systems (pulse period much larger than pulse duration).

The non-periodic component $y_{\text{NP}}(t)$ is due to the additive noise and the random transmit symbols a_k. It causes an increase of the estimation error variance. Note that this effect can be controlled by the low-pass filter bandwidth (Fig. 1). In contrast, the estimation error due to the multipath propagation is independent of the filter bandwidth. For this reason we focus on the multipath scenario in the sequel and assume $y_{\text{NP}}(t) = 0$ and $\sigma_g^2 = 0$. As our positioning system is based on the periodic component, we will analyze the impact of multipath propagation on $y_p(t)$ and on the estimator performance.

In frequency domain, the energy detector output can then be written equivalently

$$Y(f) = G(f)\frac{1}{T}\sum_{k=-\infty}^{\infty} c_k \delta\left(f - \frac{k}{T}\right),$$

where $G(f)$ denotes the transfer function of the post-detection filter and c_k the Fourier series coefficients with value

$$c_k = \int_{-\infty}^{\infty} Q(\nu)\, Q\left(\tfrac{k}{T} - \nu\right) d\nu.$$

The spectrum of the equivalent receive base pulse $q(t)$ is denoted by $Q(\nu)$.

Downconversion and low-pass filtering cuts out the Fourier coefficient c_1. The spectrum is then given by

$$Z(f) = G\left(\tfrac{1}{T}\right)\frac{1}{T}\delta(f)\int_{-\infty}^{\infty} Q(\nu)\, Q\left(\tfrac{1}{T} - \nu\right) d\nu$$

or in time domain

$$z(t) = G\left(\tfrac{1}{T}\right)\frac{1}{T}\int_{-\infty}^{\infty} Q(\nu)\, Q\left(\tfrac{1}{T} - \nu\right) d\nu. \tag{5}$$

IV. Multipath Environment

This section presents a thorough analysis of the ranging estimator according to (1) in an environment with multipath propagation. In particular, the impact of the bandwidth of the base pulse on the multipath distortion is investigated.

First, we consider the situation that the ranging system is applied in a direct LoS situation between transmitter and receiver antenna, i.e. without any multipath components. In this case, the channel induces only the desired delay of the transmit signal due to the time-of-flight according to the distance. Hence, the impulse response of the channel is given by

$$h_{\text{LOS}}(t) = \alpha_0 \cdot \delta(t - \tau_0),$$

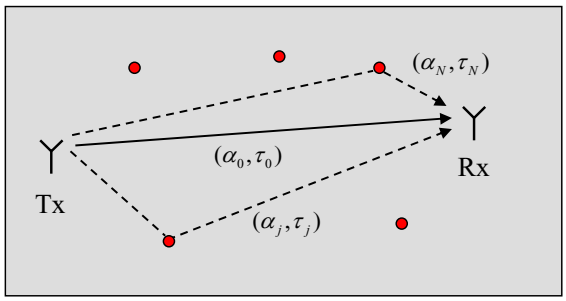

Fig. 2. Channel model with Line-of-Sight path and N scatterers

where α_0 denotes the attenuation of the radio signal and $\tau_0 = \frac{d}{c}$ the delay according to the distance d at propagation speed c.

Substituting

$$Q(f) = \tilde{P}(f) H_{\text{LOS}}(f) = \tilde{P}(f)\alpha_0 e^{-j2\pi f \tau_0}$$

into (5) leads to

$$z_{\text{LOS}}(t) = G(\tfrac{1}{T})\frac{\alpha_0^2}{T} \cdot e^{-j2\pi\frac{\tau_0}{T}} \int_{-\infty}^{\infty} \tilde{P}(\nu)\, \tilde{P}\left(\tfrac{1}{T} - \nu\right) d\nu.$$

By assumption, the spectrum of the bandpass filtered transmit base pulse $\tilde{P}(f)$ is real. The phase gives then the desired result:

$$\arg z_{\text{LOS}}(t) = -2\pi\frac{\tau_0}{T} + 2\pi\kappa, \qquad \kappa \in \mathbb{Z}.$$

This way, the distance estimator according to (1) is motivated. The ambiguity with κ translates to the ranging ambiguity of $T \cdot c$.

A. Channel Model

As depicted in Fig. 2, we apply now a channel modeling approach with one direct LoS path and N paths from scatterers or reflectors. Hence, the channel impulse response is given by

$$h(t) = \sum_{n=0}^{N} \alpha_n \delta(t - \tau_n), \tag{6}$$

where α_n and τ_n denote the path gain and path delay corresponding to the n-th path, respectively.

B. Transmit Pulse

For the ease of analysis, we choose the transmit base pulse as an ideal low-pass signal. The spectrum of the base pulse is thus given by

$$\tilde{P}(f) = \begin{cases} \frac{1}{\sqrt{B}} & \text{for } -\frac{B}{2} < f < \frac{B}{2} \\ 0 & \text{else.} \end{cases} \tag{7}$$

Certainly, this low-pass signal is not practical for radio transmission. However, extension of this analysis to bandpass transmit pulses is straightforward and leads to the same result, but expressions become lengthy then. This can also be seen by using an equivalent baseband model for the channel.

C. Estimation Bias and Variance

Given the path delays of the multipath components are uniformly i.i.d. within the pulse repetition period and the path gains are normally i.i.d. with zero-mean and variance σ_α^2, i.e.

$$\tau_n \sim \mathcal{U}(\tau_0, \tau_0 + T) \text{ and } \alpha_n \sim \mathcal{N}(0, \sigma_\alpha^2)$$

for $n = 1, \ldots, N$ and the LoS path corresponds to the parameter doublet with index 0, i.e.

$$\tau_0 = \frac{d}{c} \text{ and } \alpha_0 = \text{const.}$$

then the estimation bias is given by

$$\mathsf{E}_{\alpha,\tau}\left[\hat{d}\right] \approx -\frac{Tc}{2\pi} \arg \mathsf{E}[z(t)] = d \mod Tc$$

and the expected estimation error by

$$\mathsf{Var}_{\alpha,\tau}\left[\hat{d}\right] \approx \left(\frac{Tc}{2\pi}\right)^2 \frac{N}{\alpha_0^4}\left(\frac{3}{2}\sigma_\alpha^4 + \frac{(N-1)\sigma_\alpha^4}{BT} + \frac{2\alpha_0^2\sigma_\alpha^2}{(BT)^2}\right). \tag{8}$$

This shows that the estimator is approximately unbiased for the considered channel model. Moreover, an approximation of the estimation error is given, which shows the impact of signaling bandwidth. The approximation holds for a high LoS to multipath ratio, i.e. $\alpha_0^2 \gg \sigma_\alpha^2$, and if either the pulses are unmodulated or do not overlap (4).

This is derived as follows: Substituting the spectrum of the low-pass base pulse (7) into (5) yields at the output of downconversion

$$z(t) = G\left(\tfrac{1}{T}\right) \frac{1}{TB} \int_{-\frac{B}{2}+\frac{1}{T}}^{\frac{B}{2}} H(\nu)\, H\left(\tfrac{1}{T} - \nu\right) d\nu.$$

The integral can be written as a sum, if the signal at the input of the squarer $x(t)$ is periodic. Motivation for this assumption is that for a rather low bandwidth it is reasonable to transmit unmodulated pulses (narrowband case), i.e. $a_k = \text{const}$. For a high bandwidth (UWB), the overlapping of the pulses (intersymbol interference) is negligible. For both cases the following approximation holds with equality

$$\int_{-\frac{B}{2}+\frac{1}{T}}^{\frac{B}{2}} H(\nu)\, H\left(\tfrac{1}{T} - \nu\right) d\nu \approx \frac{1}{T} \sum_{l=-\left\lceil \frac{TB}{2} \right\rceil + 1}^{\left\lfloor \frac{TB}{2} \right\rfloor} H\left(\frac{l}{T}\right) H\left(\frac{1-l}{T}\right).$$

To get rid of the floor and ceil operation in the index boundaries and to simplify notation, we assume (without loss of generality) $\frac{TB}{2} \in \mathbb{N}$. Substituting now the spectrum of the channel impulse response (6) leads to

$$z(t) \approx G\left(\frac{1}{T}\right) \frac{1}{T^2 B} \sum_{n=0}^{N} \sum_{m=0}^{N} \alpha_n \alpha_m e^{-j2\pi \frac{1}{T}\tau_m} \cdot \sum_{l=-\frac{TB}{2}+1}^{\frac{TB}{2}} e^{-j2\pi \frac{1}{T}(\tau_n - \tau_m)l}.$$

The sum over l in the last term can be simplified with the identity

$$\sum_{l=-\frac{TB}{2}+1}^{\frac{TB}{2}} e^{-j2\pi \frac{1}{T}(\tau_n - \tau_m)l} = \begin{cases} TB & \text{for } \tau_n - \tau_m = kT \\ e^{-j\pi \frac{1}{T}(\tau_n - \tau_m)} \frac{\sin(\pi(\tau_n - \tau_m)B)}{\sin\left(\pi(\tau_n - \tau_m)\frac{1}{T}\right)} & \text{else,} \end{cases}$$

$\forall k \in \mathbb{Z}$. The output $z(t)$ can then be written compactly in matrix notation:

$$z(t) = \boldsymbol{\alpha}^T \mathbf{A} \boldsymbol{\alpha} \cdot e^{-j2\pi \frac{1}{T}\tau_0}, \tag{9}$$

where $\boldsymbol{\alpha} = [\alpha_0, \ldots, \alpha_N]^T$ and

$$\mathbf{A} = \begin{bmatrix} 1 & a_{01} & \cdots & a_{0N} \\ a_{10} & e^{-j2\pi \frac{\tau_1 - \tau_0}{T}} & \ddots & \vdots \\ \vdots & \ddots & \ddots & a_{(N-1)N} \\ a_{N0} & \cdots & a_{N(N-1)} & e^{-j2\pi \frac{\tau_N - \tau_0}{T}} \end{bmatrix} \frac{G(\frac{1}{T})}{T}$$

with

$$a_{n,m} = \frac{1}{TB} e^{-j\pi \frac{1}{T}(\tau_n + \tau_m - \tau_0)} \frac{\sin(\pi(\tau_n - \tau_m)B)}{\sin\left(\pi(\tau_n - \tau_m)\frac{1}{T}\right)}.$$

Estimation Bias: Linearization of $\arg(\cdot)$ yields for small variances

$$\mathsf{E}[\arg z(t)] \approx \arg \mathsf{E}[z(t)].$$

Using (9), the phase of the expectation of the downconversion output $z(t)$ can be written as

$$\arg \mathsf{E}[z(t)] = \left(\arg e^{-j2\pi \frac{\tau_0}{T}} + \arg \mathsf{E}_{\alpha,\tau}\left[\boldsymbol{\alpha}^T \mathbf{A} \boldsymbol{\alpha}\right]\right) \bmod 2\pi.$$

The expectation of the quadratic form yields[1]

$$\mathsf{E}_{\alpha,\tau}\left[\boldsymbol{\alpha}^T \mathbf{A} \boldsymbol{\alpha}\right] = \mathrm{Tr}\left(\mathsf{E}_\tau[\mathbf{A}]\boldsymbol{\Sigma}\right) + \boldsymbol{\mu}^T \mathsf{E}_\tau[\mathbf{A}]\boldsymbol{\mu}, \tag{10}$$

where

$$\boldsymbol{\mu} = \mathsf{E}[\boldsymbol{\alpha}] = [\alpha_0, 0, \ldots, 0]^T$$

and

$$\boldsymbol{\Sigma} = \mathsf{Cov}[\boldsymbol{\alpha}] = \mathrm{diag}\left([0, \sigma_\alpha^2, \ldots, \sigma_\alpha^2]^T\right).$$

The expectation of $\mathbf{A}$ with respect to τ yields

$$\mathsf{E}_\tau[\mathbf{A}] = \mathrm{diag}\left([1, 0, \ldots, 0]^T\right) \frac{G\left(\frac{1}{T}\right)}{T}.$$

Substituting this, the expectation (10) then computes to

$$\mathsf{E}_{\alpha,\tau}\left[\boldsymbol{\alpha}^T \mathbf{A} \boldsymbol{\alpha}\right] = \alpha_0^2 \frac{G\left(\frac{1}{T}\right)}{T}.$$

Since it is assumed that the transfer function of the post detection filter $g(t)$ is real, it follows

$$\arg \mathsf{E}_{\alpha,\tau}[\boldsymbol{\alpha}^T \mathbf{A} \boldsymbol{\alpha}] = 0$$

[1] cf. [11]: Let $\boldsymbol{\alpha} \sim \mathcal{N}(\boldsymbol{\mu}, \boldsymbol{\Sigma})$, $\boldsymbol{\Lambda} \in \mathbb{R}^{N+1 \times N+1}$ and symmetric, then $\mathsf{E}[\boldsymbol{\alpha}^T \boldsymbol{\Lambda} \boldsymbol{\alpha}] = \mathrm{Tr}[\boldsymbol{\Lambda}\boldsymbol{\Sigma}] + \boldsymbol{\mu}^T \boldsymbol{\Lambda} \boldsymbol{\mu}$ and $\mathsf{Var}[\boldsymbol{\alpha}^T \boldsymbol{\Lambda} \boldsymbol{\alpha}] = 2\mathrm{Tr}[\boldsymbol{\Lambda}\boldsymbol{\Sigma}\boldsymbol{\Lambda}\boldsymbol{\Sigma}] + 4\boldsymbol{\mu}^T \boldsymbol{\Lambda}\boldsymbol{\Sigma}\boldsymbol{\Lambda}\boldsymbol{\mu}$.

and further

$$\arg \mathsf{E}[z(t)] = \frac{2\pi}{Tc}\,(d \mod Tc)\,.$$

Thus, the estimator is approximately unbiased for this channel model.

Error Variance: Applying again linearization of $\arg(\cdot)$ yields for $\alpha_0^2 \gg \sigma_\alpha^2$ for the expected estimation error

$$\begin{aligned}\mathsf{Var}_{\alpha,\tau}\left[\hat{d}\right] &= \left(\tfrac{Tc}{2\pi}\right)^2 \mathsf{Var}[\arg \boldsymbol{\alpha}^T \mathbf{A}\boldsymbol{\alpha}] \\ &\approx \left(\tfrac{Tc}{2\pi}\right)^2 \frac{\mathsf{E}[\mathrm{Im}\left\{\boldsymbol{\alpha}^T\mathbf{A}\boldsymbol{\alpha}\right\}^2]}{|\mathsf{E}\left[\boldsymbol{\alpha}^T\mathbf{A}\boldsymbol{\alpha}\right]|^2}.\end{aligned}$$

The second moment of the imaginary part of the quadratic form $\boldsymbol{\alpha}^T\mathbf{A}\boldsymbol{\alpha}$ can be written as[1]

$$\begin{aligned}&\mathsf{E}_{\alpha,\tau}\left[\mathrm{Im}\left\{\boldsymbol{\alpha}^T\mathbf{A}\boldsymbol{\alpha}\right\}^2\right] \\ &= \mathsf{E}_\tau\left[2\mathrm{Tr}\left[\left(\mathrm{Im}\left\{\mathbf{A}\right\}\boldsymbol{\Sigma}\right)^2\right] + 4\boldsymbol{\mu}^T\mathrm{Im}\left\{\mathbf{A}\right\}\boldsymbol{\Sigma}\mathrm{Im}\left\{\mathbf{A}\right\}\boldsymbol{\mu} + \right. \\ &\qquad \left. + \left(\mathrm{Tr}\left[\left(\mathrm{Im}\left\{\mathbf{A}\right\}\boldsymbol{\Sigma}\right)\right] + \boldsymbol{\mu}^T\mathrm{Im}\left\{\mathbf{A}\right\}\boldsymbol{\mu}\right)^2\right] \\ &= 2\sigma_\alpha^4\sum_{n=1}^{N}\sum_{m=1}^{N}\mathsf{E}_\tau\left[\mathrm{Im}\left\{\mathbf{A}_{n,m}\right\}^2\right] + \sum_{n=1}^{N}\mathsf{E}_\tau\left[\mathrm{Im}\left\{\mathbf{A}_{n,n}\right\}^2\right] + \\ &\qquad + 4\alpha_0^2\sigma_\alpha^2\sum_{m=1}^{N}\mathsf{E}_\tau\left[\mathrm{Im}\left\{\mathbf{A}_{0,m}\right\}^2\right].\end{aligned}$$

The expectation with respect to τ computes to:

i) For $n = m$:

$$\mathsf{E}_\tau\left[\mathrm{Im}\left\{\mathbf{A}_{n,n}\right\}^2\right] = \mathsf{E}_\tau\left[\left(\frac{G\left(\frac{1}{T}\right)}{T}\sin\left(2\pi\tfrac{\tau_n}{T}\right)\right)^2\right] = \frac{G^2\left(\frac{1}{T}\right)}{2T^2}$$

ii) For $n \neq m$:

$$\begin{aligned}&\mathsf{E}_\tau\left[\mathrm{Im}\left\{\mathbf{A}_{n,m}\right\}^2\right] = \\ &= \mathsf{E}_\tau\left[\left(\frac{G\left(\frac{1}{T}\right)}{T^2B}\frac{\sin(\pi(\tau_n+\tau_m)\frac{1}{T})\sin(\pi(\tau_n-\tau_m)B)}{\sin\left(\pi(\tau_n-\tau_m)\frac{1}{T}\right)}\right)^2\right] = \frac{G^2\left(\frac{1}{T}\right)}{2T^3B}\end{aligned}$$

iii) For $n = 0 \neq m$:

$$\mathsf{E}_\tau\left[\mathrm{Im}\left\{\mathbf{A}_{0,m}\right\}^2\right] = \mathsf{E}_\tau\left[\left(\frac{G\left(\frac{1}{T}\right)}{T^2B}\sin\left(\pi\tau_m B\right)\right)^2\right] = \frac{G^2\left(\frac{1}{T}\right)}{2T^4B^2}$$

Collecting terms yields

$$\frac{\mathsf{E}\left[\mathrm{Im}\left\{\boldsymbol{\alpha}^T\mathbf{A}\boldsymbol{\alpha}\right\}^2\right]}{|\mathsf{E}\left[\boldsymbol{\alpha}^T\mathbf{A}\boldsymbol{\alpha}\right]|^2} = \frac{N}{\alpha_0^4}\left(\frac{3}{2}\sigma_\alpha^4 + \frac{(N-1)\sigma_\alpha^4}{BT} + \frac{2\alpha_0^2\sigma_\alpha^2}{(BT)^2}\right)$$

and finally leads to (8).

Expression (8) shows the influence of the bandwidth of the transmit pulse on the estimation accuracy. The higher the bandwidth of the transmit pulse, the better becomes the ranging accuracy. However, there is an error floor that is determined by the term $\frac{3}{2}\sigma_\alpha^4$, which is independent of B. The second term scales with $\frac{1}{BT}$ and corresponds to overlap of the multipath terms. The higher the bandwidth, the shorter are the pulses and therefore the probability of overlap decreases. The third term scales with $\frac{1}{(BT)^2}$ and is related to the overlap of multipath components with the LoS path.

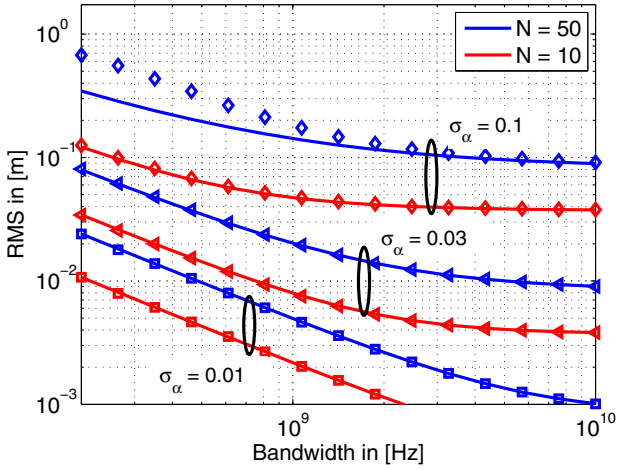

Fig. 3. Simulation (markers) and approximation (lines) of RMS of ranging error vs. bandwidth for channel model ($\frac{1}{T} = 50$ MHz).

V. Performance Results

This section presents the performance analysis of the proposed ToA estimator. First, the estimation error according to (8) is compared to Monte Carlo simulation. Second, the estimation error and bias is evaluated for a rich multipath indoor environment based on measured channel impulse responses. The pulse repetition frequency has been chosen to $\frac{1}{T} = 50$ MHz, i.e. the uncertainty window is 6 m. This would be an adequate value e.g. for motion tracking of human body parts. As figure of merit, we consider the root mean square of the estimation error.

Fig. 3 depicts the influence of the bandwidth of the transmit pulse according to (8). The RMS is plotted for different values of σ_α and number of scatterers N. The magnitude of the direct LoS path is set to $\alpha_0 = 1$. The solid lines correspond to the analytical result and show very good matching compared to the Monte Carlo simulation (markers) for sufficiently small σ_α. This validates the approximations in Section IV in the derivation of the expected estimation error. The result shows how the positioning accuracy increases with increasing bandwidth. In particular, the $\frac{1}{B}$-scaling of the estimation error can be seen in Fig. 3 for the small value of σ_α. However, the estimation accuracy saturates at a certain error floor, which is given by the bandwidth independent term in (8).

For the performance evaluation based on measured channel impulse responses two different scenarios are chosen: a typical LoS situation and a non-LoS situation in an indoor environment with rich multipath propagation. Fig. 4 shows the estimation bias versus bandwidth and Fig. 5 the RMS based on 8820 LoS measurements and 5020 non-LoS measurements for bandpass signaling with center frequency $f_c = 4.5$ GHz. The measurement setup and postprocessing is described in detail in [12]. The results show that the estimation bias is small for a sufficient bandwidth. For the LoS situation, the positioning error saturates at about 20 cm compared to 30 cm for the

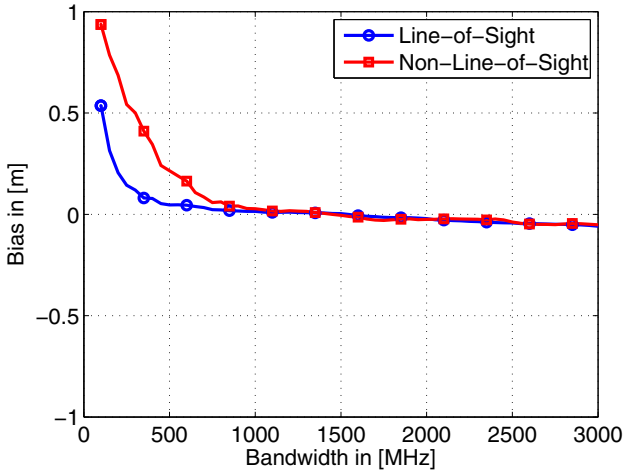

Fig. 4. Bias of ranging estimate vs. bandwidth for measured channels.

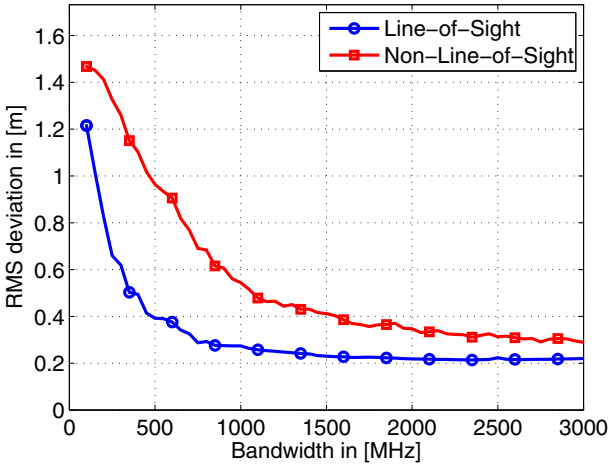

Fig. 5. RMS of ranging error vs. bandwidth for measured channels.

non-LoS case. However, for a low signaling bandwidth, the estimation performance is very poor. The upper limit of the y-axis in Fig. 5 is set to $\sqrt{3}$ m $\approx$ 1.73 m, which would correspond to the RMS of uniformly distributed guessing in the uncertainty window of 6 m. This shows that in this environment the phase of narrowband signals is almost useless for positioning and narrowband systems would not give a reliable position estimate. In contrast, when using UWB pulses with a bandwidth of 2 GHz or more the systems performance is improved substantially.

VI. Summary

Low complexity position estimation based on UWB energy detection and spectral estimation has been presented and analyzed. Moreover, the influence of the bandwidth is investigated and a closed form approximation of the estimation variance is presented. Performance evaluation based on measured channel impulse responses show that up to 20 cm accuracy can be reached.

References

[1] H. Fan and C. Yan, "Asynchronous differential TDOA for sensor self-localization," in *IEEE International Conference on Acoustics, Speech and Signal Processing, 2007. ICASSP 2007*, vol. 2, April 2007, pp. II–1109–II–1112.

[2] E. D. Kaplan, *Understanding GPS: Principles and Applications*. Artech House, 1996.

[3] K. Pahlavan, X. Li, and J. Makela, "Indoor geolocation science and technology," *IEEE Communications Magazine*, vol. 40, no. 2, pp. 112–118, Feb 2002.

[4] S. Gezici, Z. Tian, G. Giannakis, H. Kobayashi, A. Molisch, H. Poor, and Z. Sahinoglu, "Localization via ultra-wideband radios: a look at positioning aspects for future sensor networks," *IEEE Signal Processing Magazine*, vol. 22, no. 4, pp. 70–84, July 2005.

[5] S. Aedudodla, S. Vijayakumaran, and T. Wong, "Timing acquisition in ultra-wideband communication systems," *IEEE Transactions on Vehicular Technology*, vol. 54, no. 5, pp. 1570–1583, Sept. 2005.

[6] J.-Y. Lee and R. Scholtz, "Ranging in a dense multipath environment using an UWB radio link," *IEEE Journal on Selected Areas in Communications*, vol. 20, no. 9, pp. 1677–1683, Dec 2002.

[7] D. Dardari, C.-C. Chong, and M. Win, "Threshold-based time-of-arrival estimators in UWB dense multipath channels," *IEEE Transactions on Communications*, vol. 56, no. 8, pp. 1366–1378, August 2008.

[8] I. Guvenc, Z. Sahinoglu, and P. Orlik, "TOA estimation for IR-UWB systems with different transceiver types," *IEEE Transactions on Microwave Theory and Techniques*, vol. 54, no. 4, pp. 1876–1886, June 2006.

[9] H. Luecken, C. Steiner, and A. Wittneben, "ML timing estimation for generalized UWB-IR energy detection receivers," in *IEEE International Conference on Ultra-Wideband, ICUWB 2009*, Sept. 2009, pp. 829–833.

[10] M. Oerder and H. Meyr, "Digital filter and square timing recovery," *IEEE Transactions on Communications*, vol. 36, no. 5, pp. 605–612, May 1988.

[11] A. C. Rencher and G. B. Schaalje, *Linear Models in Statistics*, 2nd ed. John Wiley & Sons, Inc, 2008.

[12] F. Althaus, F. Troesch, T. Zasowski, and A. Wittneben, "STS measurements and characterization," *PULSERS Deliverable D3b6a*, vol. IST-2001-32710 PULSERS, 2005.